Electronic Supplementary Information

Phosphorus-doped hard carbon with controlled active groups and microstructure for high-performance sodium-ion batteries

Na Li*[a], Qianya Yang[a], Yanxin Wei[a], Richuan Rao[a], Yanping Wang[a], Maolin Sha[a], Xiaohang Ma[a], Lili Wang*[b], Yitai Qian[c]

a. Department of Chemical and Chemical Engineering, Hefei normal University, Hefei, Anhui 230601, PR China，E-mail: sdjnlina@163.com.

b. School of Energy, Materials and Chemical Engineering, Hefei University, Hefei, Anhui 230601, P. R. China, E-mail: wangll@hfuu.edu.cn.

c. Department of Applied Chemistry, University of Science and Technology of China, Hefei 230026, P. R. China.

Supporting Figures

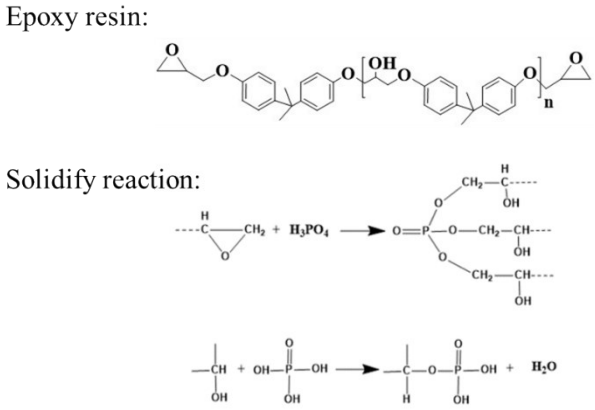

Fig. S1. The corresponding reactions between epoxy resin and H_3PO_4.

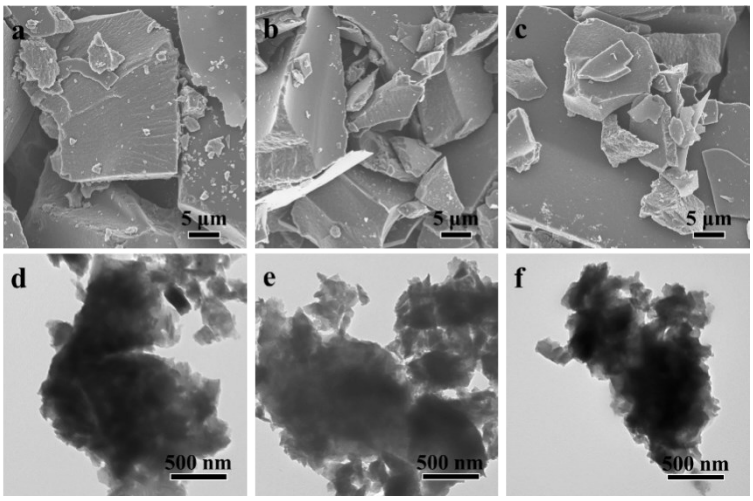

Fig. S2. SEM images of a) PHC-500, b) PHC-700, c) PHC-900. TEM images of d) PHC-500, e) PHC-700, f) PHC-900.

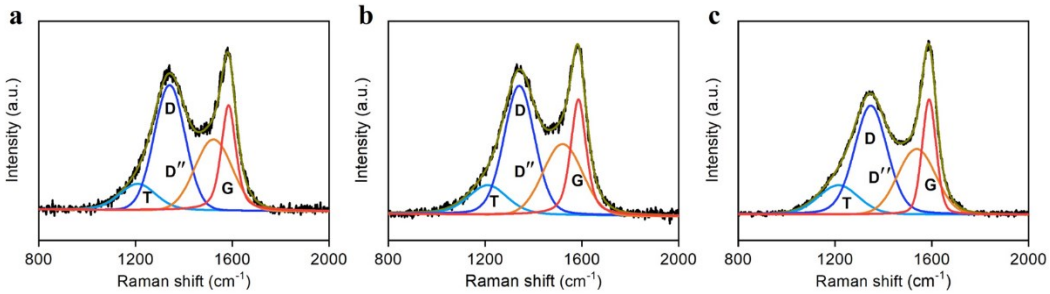

Fig. S3. Fitted Raman spectra curves of a) PHC-500, b) PHC-700, c) PHC-900. The blue line with a peak at 1360 cm^{-1} represents the D-band, while the red line with a peak close to 1585 cm^{-1} represents the G-band. Integrated ratios are obtained from the area of the fitted peaks. The fitting is made using the OMINC Picta software program with a guassian-laurenztian fit.[1]

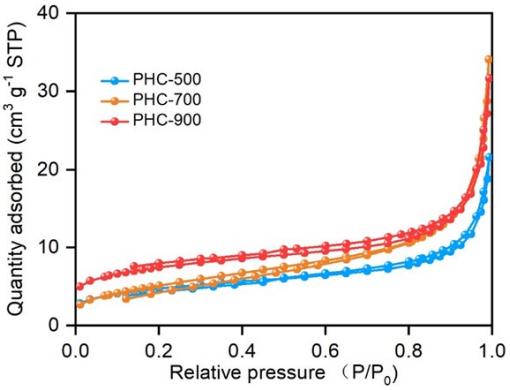

Fig. S4. Nitrogen adsorption-desorption isotherms of PHC-500, PHC-700 and PHC-900.

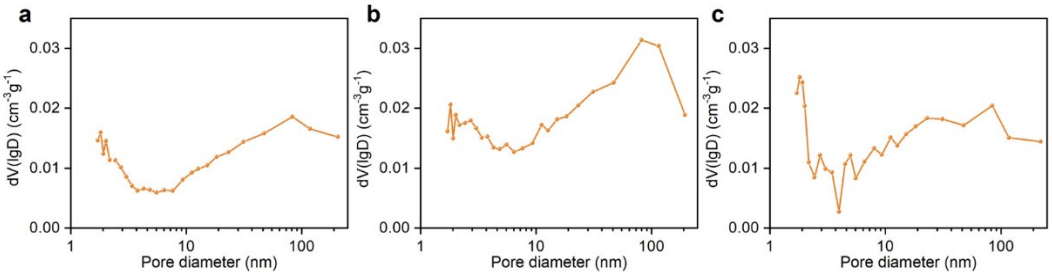

Fig. S5. Pore-size distribution of a) PHC-500, b) PHC-700 and c) PHC-900.

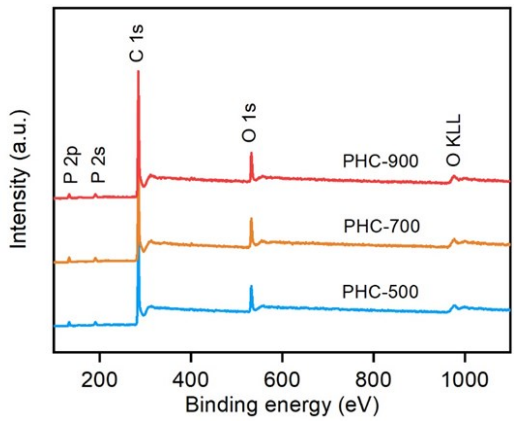

Fig. S6. XPS survey scans of PHC-500, PHC-700 and PHC-900.

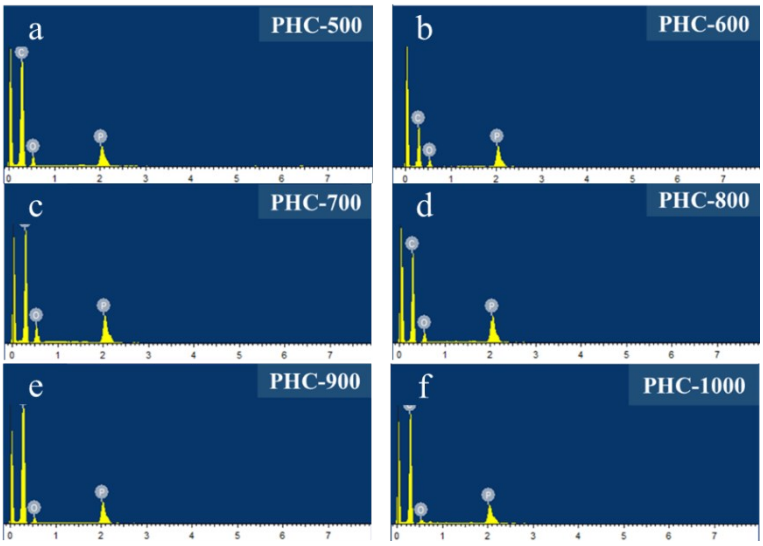

Fig. S7. EDS elemental analysis and contents of a) PHC-500, b) PHC-600, c) PHC-700, d) PHC-800, e) PHC-900, f) PHC-1000.

Table S1. Structure parameters and elemental compositions of PHC-Ts at different temperatures.

Sample	L_a[1] [nm]	L_c[2] [nm]	N[3]	V [cm^3/g]	ρ [g/cm^3]	EDS at.% C	O	P
PHC-500	4.59	0.97	2.66	0.033	1.144	83.85	12.38	3.77
PHC-600	4.88	0.98	2.68	0.034	1.141	84.07	11.40	4.53
PHC-700	5.01	1.07	2.69	0.042	1.127	84.99	9.60	5.41
PHC-800	5.16	1.06	2.77	0.049	1.109	86.60	9.10	4.30
PHC-900	5.52	1.13	2.98	0.053	1.063	88.02	8.09	3.89
PHC-1000	5.99	1.15	3.04	0.027	1.203	88.82	7.43	3.75

Note: L_a[1] (nm) = $(2.4 * 10^{-10})\ \lambda_{nm}^4 (I_G/I_D)$; L_c[2] (nm) = $0.89\lambda/(t\cos\theta)$; N[3] = $L_c/d_{(002)} + 1$. The tap density is measured by JZ-1 powder compaction density meter (Chengdu Jingxin Powder Testing Equipment Co., Ltd).

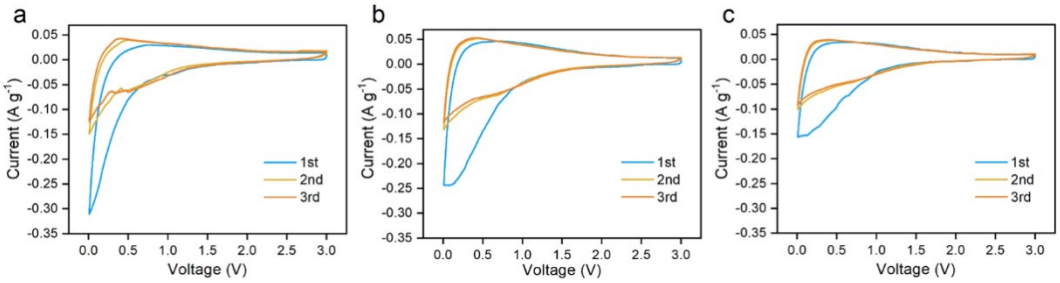

Fig. S8. CV curves at a scan rate of 0.1 mV s^{-1} of a) PHC-500, b) PHC-700, c) PHC-900.

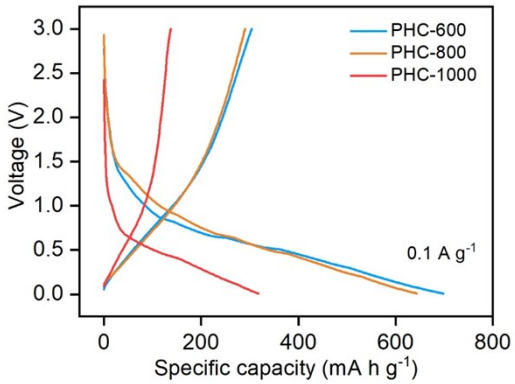

Fig. S9. Galvanostatic first discharge/charge profiles at current rate of 0.1 A g^{-1} of PHC-600, PHC-800, PHC-1000.

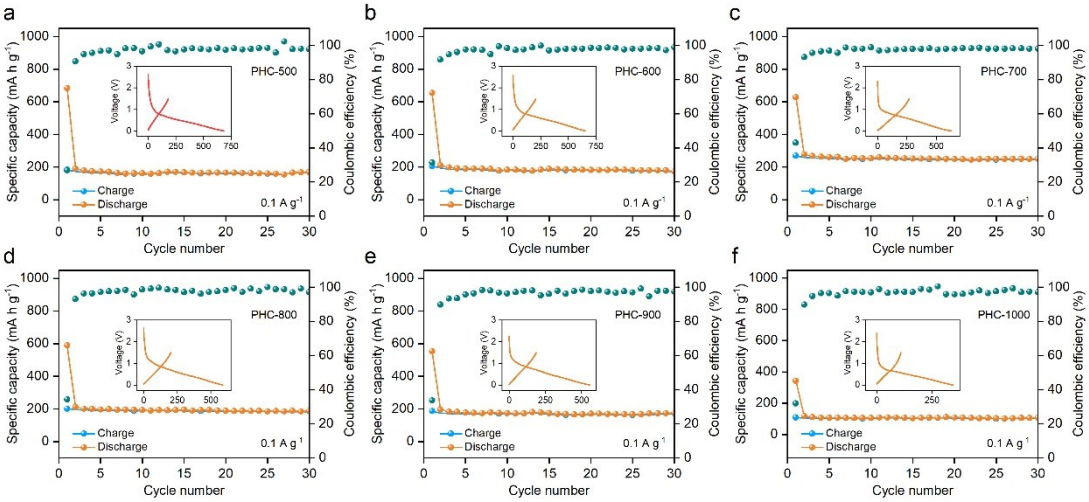

Fig. S10. The electrochemical performances of PHC-Ts between 0.01-1.5 V at 100 mA g^{-1} of a) PHC-500, b) PHC-600, c) PHC-700, d) PHC-800, e) PHC-900 and f) PHC-1000.

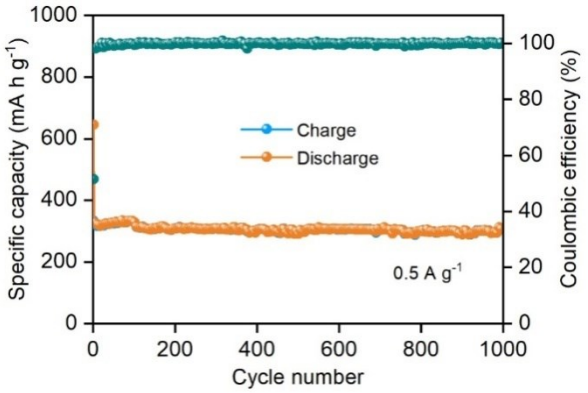

Fig. S11. Cycling performance of PHC-700 at current rate of 0.5 A g^{-1}.

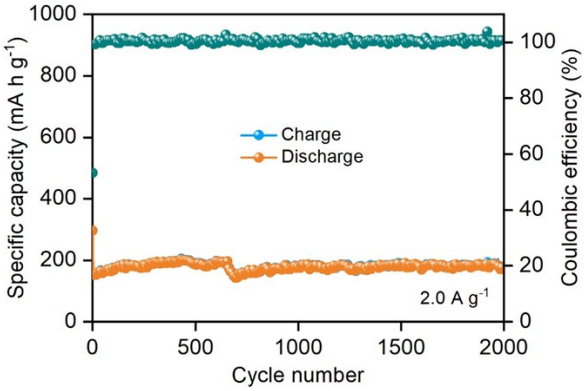

Fig. S12. Cycling performance of PHC-700 at current rate of 2.0 A g^{-1}.

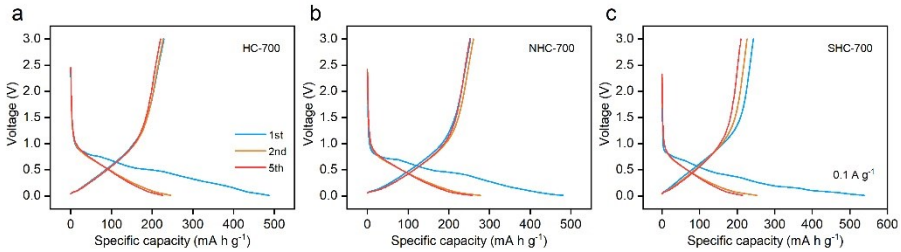

Fig. S13. The charge/discharge curves at 1st, 2nd and 5th with current density of 100 mA g^{-1} for a) HC-700, b) NHC-700 and c) SHC-700.

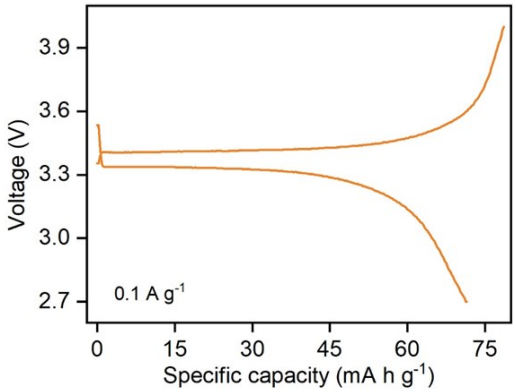

Fig. S14. Galvanostatic first discharge/charge profiles at current rate of 0.1 A g^{-1} of $Na_3V_2(PO_4)_3$ cathode.

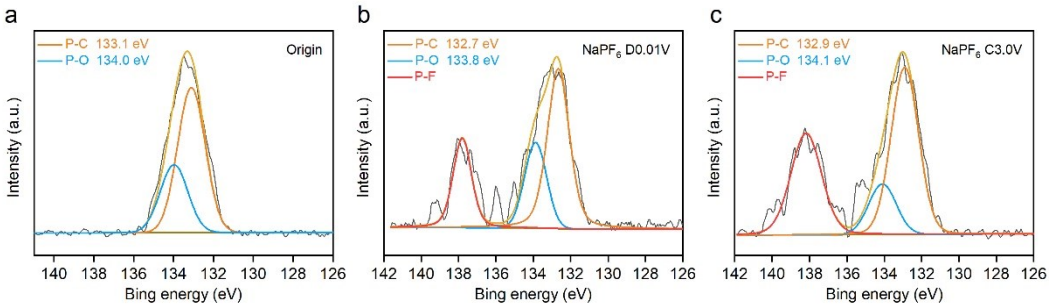

Fig. S15. The high-resolution P 2p spectra of PHC-700 electrode with $NaPF_6$ electrolyte at different charge/discharge states of a) origin, b) D0.01V and c) C3.0V.

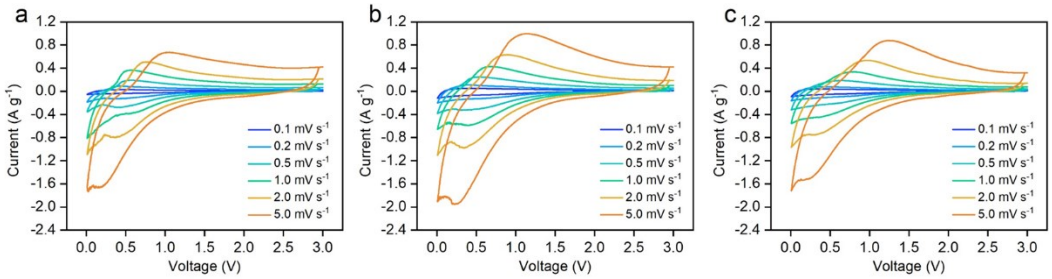

Fig. S16. CV curves at various scan rates of a) PHC-500, b) PHC-700, c) PHC-900.

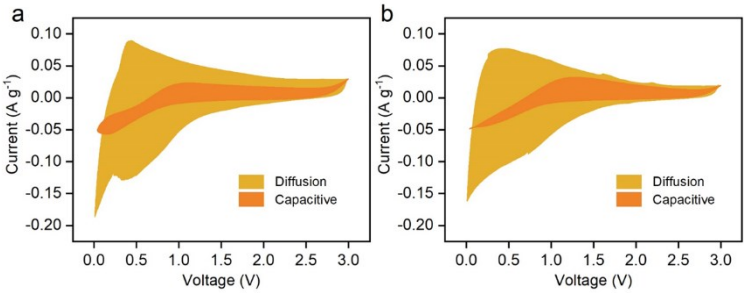

Fig. S17. Capacitive contribution at the scan rate of 0.2 mV s^{-1} of a) PHC-500 and b) PHC-900.

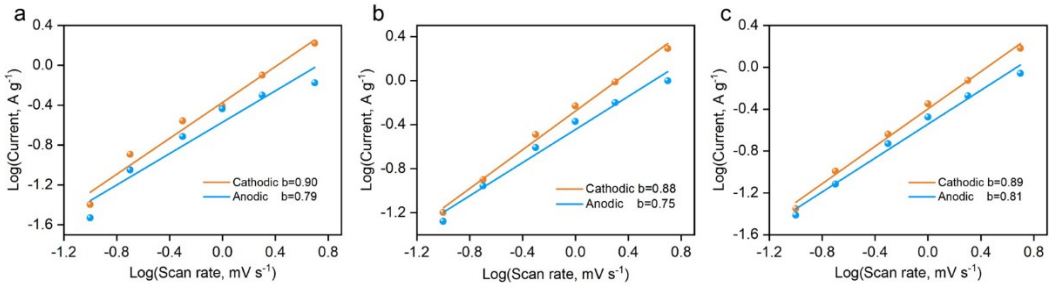

Fig. S18. Liner relationship between the peak current and scan rates in logarithmic format of a) PHC-500, b) PHC-700 and c) PHC-900.

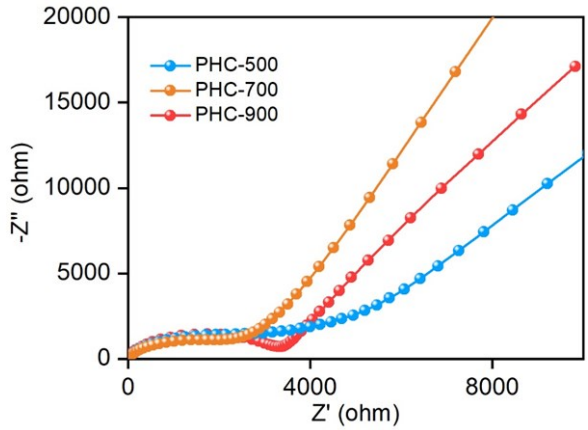

Fig. S19. Nyquist plots of the PHC-500, PHC-700 and PHC-900.

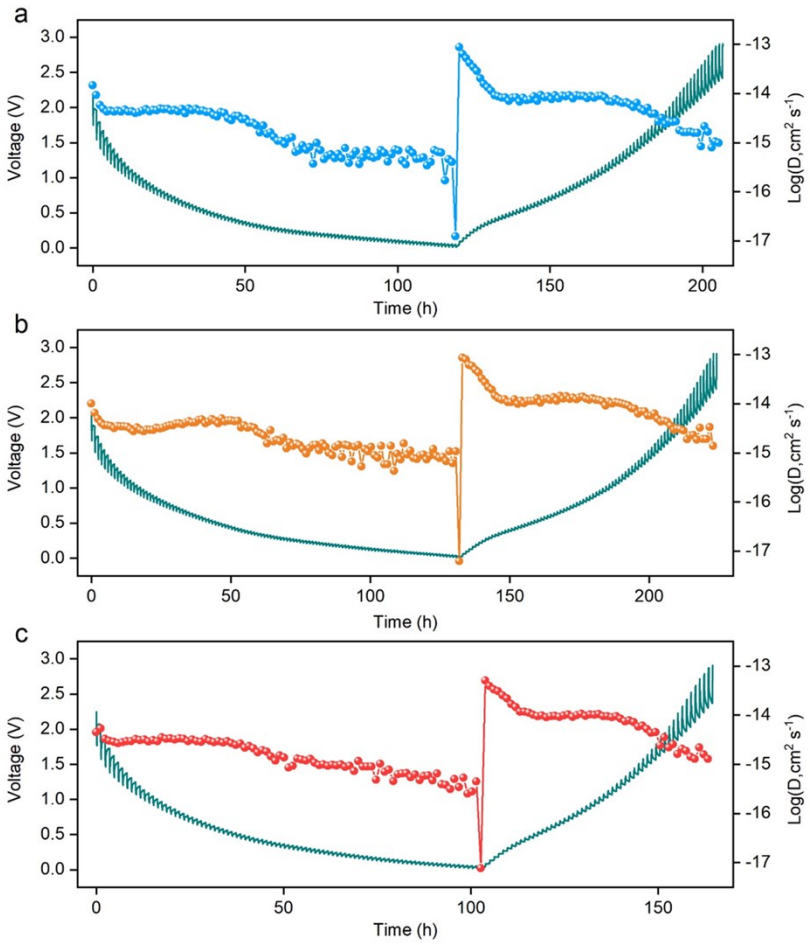

Fig. S20. The GITT curves and the corresponding Na-ion diffusion coefficients calculated from the GITT curves as a function of time during discharge/charge processes of a) PHC-500, b) PHC-700 and c) PHC-900.

Ion diffusivity is a key factor of electrode materials for batteries, which links directly to their rate capability. In order to study the influence of the temperature on the ion diffusion coefficients, the GITT method is carried out to measure the PHC-500, PHC-700 and PHC-900 samples. Based on the GITT measurement, the lithium diffusion coefficients can be calculated by the following equation:[2]

$$D_{Na^+} = \frac{4}{\pi}(\frac{m_B V_M}{M_B S})^2(\frac{\Delta E_S}{\tau(dE_\tau / d\sqrt{\tau})})^2 .....(\tau << L^2 / D_{Na^+})$$

Where V_M (cm^3 mol^{-1}) is the molar volume of samples, M_B (g mol^{-1}) and m_B (g) are the molecular weight and mass of the electrode materials, respectively. S (cm^2) is the active surface area of the electrode, which is measured by the BET method. L (cm) is the diffusion distance, which is approximately the thickness of the electrode. The equation could be further simplified as:[3]

$$D_{Na^+} = \frac{4}{\pi\tau}(\frac{m_B V_M}{M_B S})^2(\frac{\Delta E_S}{\Delta E_\tau})^2$$

Supporting References:

1. A. Sadezky, H. Muckenhuber, H. Grothe, R. Niessner and U. Pöschl, Carbon, 2005, 43, 1731-1742.

2. W. Weppner and R. A. Huggins, Journal of The Electrochemical Society, 1977, 124, 1569-1578.

3. K. Shaju, G. S. Rao and B. Chowdari, Electrochimica Acta, 2003, 48, 2691-2703.